Proceedings of INMM & ESARDA Joint Annual Meeting
May 22–26, 2023

Solving the Rubik's Cube: two dimensional neutron radiography with superheated droplet detectors

Jihye Jeon[1], Andrew Gilbert[2], Erik P. Gilson[3], Alexander Glaser[1], Robert Goldston[1,3]

[1]*Princeton University, Princeton, NJ 08544*
[2]*Pacific Northwest National Laboratory, Richland, WA 99354*
[3]*Princeton Plasma Physics Laboratory, Princeton, NJ 08543*

Abstract. We have previously studied Zero-Knowledge-Protocol (ZKP) differential neutron radiography for warhead verification, using superheated droplet (bubble) detectors. We successfully showed the proof-of-concept using one dimensional radiography experiments. In the present study, we conducted calculations and preliminary experiments with a test object with full 3D structure (4×4×4 = 64 voxels) combined with 2D radiography. The baseline target object is a (4"×4"×4") cube, which consists of eight 1" stainless steel cubes (2×2×2 = 8 voxels) in the center surrounded by 58 1" high density polyethylene cubes. We swapped some of steel cubes with aluminum and polyethylene blocks to test the sensitivity of the system. A total of 16 bubble detectors were located behind the target in a (4×4) grid. We used 14 MeV neutrons coming from the "EXCALIBUR" neutron source available at the Princeton Plasma Physics Laboratory, which allows rapid measurements. Theoretically, measurements from two sides should provide enough data to solve for the opacity of the 8 central blocks. Initial experimental results are in reasonable agreement with MCNP calculations for the overall bubble count rates, and general trends can be seen. Results with higher total counts and accurate inter-detector calibration will be presented.

Introduction

In arms control treaty verification, the Host, whose weapons are under inspection, will require high confidence without revealing any information about the configuration or composition of their warheads. On the other hand, the Inspector will want to confirm with high confidence whether or not inspected items are real nuclear warheads.

To address these concerns, our group previously introduced a Zero-Knowledge Protocol (ZKP) differential radiography approach for warhead verification.[1] We showed that superheated emulsion, droplet or bubble detectors, can be used for this application by demonstrating the proof-of-concept using one dimensional radiography experiments.[2] In this study, we conducted calculations and preliminary experiments with a test object with full 3D structure ($4\times4\times4 = 64$ voxels) combined with 2D radiography.

Methods

2D radiography with bubble detectors

For 2D radiography, we used the EXCALIBUR (EXperiment for CALIBration with URanium) neutron source available at the Princeton Plasma Physics Laboratory (PPPL).[3] The EXCALIBUR has a D-T generator, and it allows us to use the direct 14 MeV neutrons through its fan-shaped collimator. As shown in the Figure 1, we test a (4"×4"×4") cube, which consists of eight 1" cubes of stainless steel 304 or aluminum cubes ($2\times2\times2 = 8$ voxels) in the center surrounded by 58 1" high density polyethylene cubes. A total of 16 bubble detectors were located behind the target in a (4×4) grid. We placed the target at 1.1 m and detectors at 1.6 m from the neutron source, so that we can give some space around the target, assuming that it could be in a container.

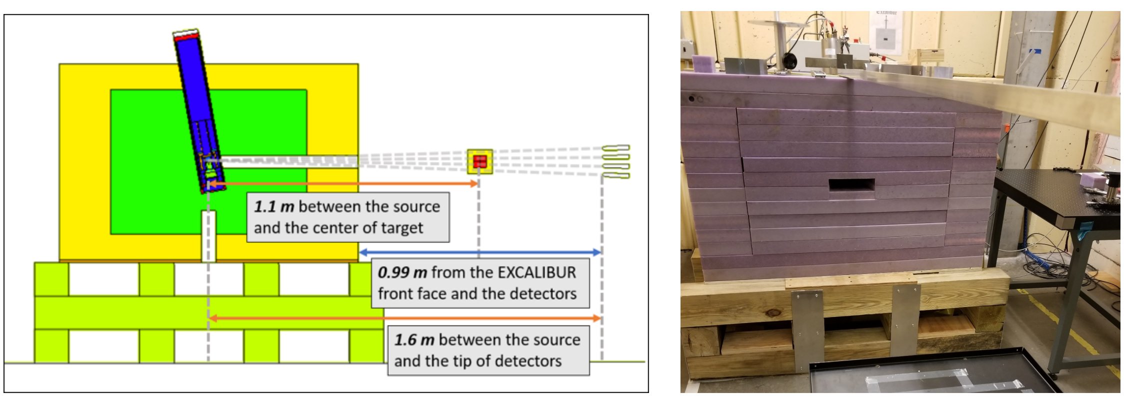

Figure 1: (Left) MCNP6 model for 2D radiography with the EXCALIBUR neutron source, a 4×4×4 voxel target and bubble detectors in a 4×4 grid. (Right) A picture of the EXCALIBUR source at PPPL.

To test the sensitivity of the system, we swapped some of steel cubes in the center with aluminum and came up with three different target configurations as shown in Figure 2. In this study, we only focused on the bottom four blocks in the center.

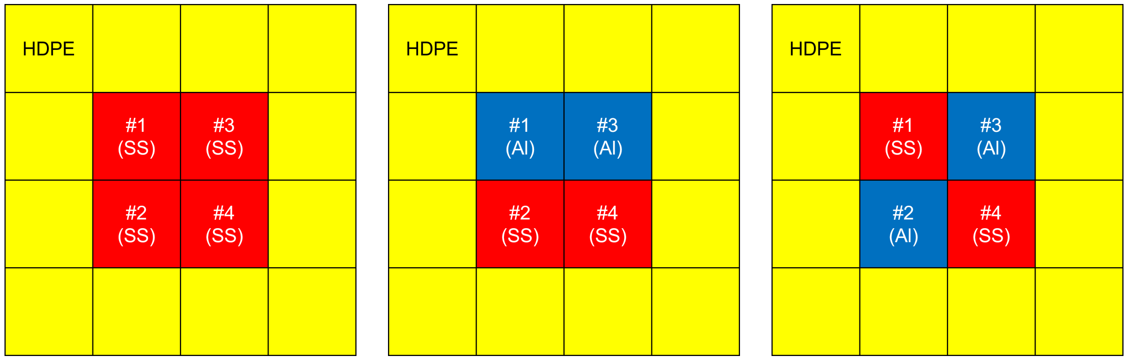

(a) case 1 (b) case 2 (c) case 3

Figure 2: Three cases of target configurations. The picture shows the top view of the bottom four stainless steel (red) or aluminum (blue) blocks in the center surrounded by high density polyethylene blocks (yellow). All block are in a shape of 1" cube.

Linear algebraic model for solving the cube

For the simplicity of the problem, we assumed:

- S_i: bubble counts of detector i
- R: bubble detector response function. $R \approx 10^{-3}$ at 14 MeV.
- ϕ_0: incoming neutron flux. We supposed the neutron flux is the same everywhere on the cube face.
- Σ_i: neutron total cross-section (inch^{-1}) of block i at 14 MeV. We supposed we know the $\Sigma_{poly} = 0.272$ inch^{-1}.
- x_i: neutron path length (inch) of block i. We supposed we know that the Rubik's cube consists of 1" blocks.

Our goal here is to discern blocks with different material in the center based on the measurements results $S_1 - S_6$. We can have a simple neutron attenuation equation, supposing the group A includes the blocks neutrons are going through:

$$\phi = \phi_0 exp(-\sum_{j \in A} x_j \Sigma_j)$$

$$S_i = R(\phi) \approx 10^{-3} \phi_0 exp(-\sum_{j \in A} x_j \Sigma_j)$$

Figure 3 shows the possible measurement scheme.

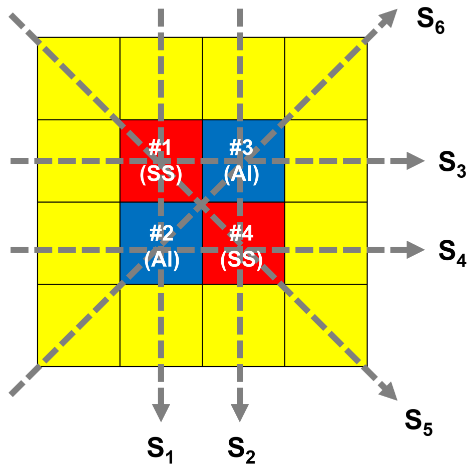

Figure 3: Possible neutron measurements for the case 3 in Figure 2. Gray dotted lines show the neutron path through four blocks (two poly and two center blocks) and $S_1 - S_6$ denotes the number of bubbles (signals) looking at those attenuated neutrons.

Using the general equation above, we can write:

$$S_1 = 10^{-3}\phi_0 exp(-2\Sigma_{poly} - \Sigma_1 - \Sigma_2)$$
$$S_2 = 10^{-3}\phi_0 exp(-2\Sigma_{poly} - \Sigma_3 - \Sigma_4)$$
$$\vdots$$
$$S_5 = 10^{-3}\phi_0 exp(-2\sqrt{2}\Sigma_{poly} - \sqrt{2}\Sigma_1 - \sqrt{2}\Sigma_4)$$
$$S_6 = 10^{-3}\phi_0 exp(-2\sqrt{2}\Sigma_{poly} - \sqrt{2}\Sigma_2 - \sqrt{2}\Sigma_3)$$

This set of equations can be expressed as a linear algebra problem when taking log on both sides:

$$\begin{pmatrix} ln(S_1) \\ ln(S_2) \\ ln(S_3) \\ ln(S_4) \\ ln(S_5) \\ ln(S_6) \end{pmatrix} = \begin{pmatrix} -3ln(10) + ln(\phi_i) - 2\Sigma_{poly} \\ -3ln(10) + ln(\phi_i) - 2\Sigma_{poly} \\ -3ln(10) + ln(\phi_i) - 2\Sigma_{poly} \\ -3ln(10) + ln(\phi_i) - 2\Sigma_{poly} \\ -3ln(10) + ln(\phi_i) - 2\sqrt{2}\Sigma_{poly} \\ -3ln(10) + ln(\phi_i) - 2\sqrt{2}\Sigma_{poly} \end{pmatrix} - \underbrace{\begin{pmatrix} 1 & 1 & 0 & 0 \\ 0 & 0 & 1 & 1 \\ 1 & 0 & 1 & 0 \\ 0 & 1 & 0 & 1 \\ \sqrt{2} & 0 & 0 & \sqrt{2} \\ 0 & \sqrt{2} & \sqrt{2} & 0 \end{pmatrix}}_{A} \begin{pmatrix} \Sigma_1 \\ \Sigma_2 \\ \Sigma_3 \\ \Sigma_4 \end{pmatrix}$$

Since we have only four unknowns, $\Sigma_1 - \Sigma_4$, one can ask why not use four equations instead of six, which will give us a simple four by four matrix, not six by four matrix like above. However, we need to be careful when we choose four signals out of six in Figure 3. Figure 3, with the case 3 from Figure 2, shows the perfect example as a cheating scenario with not-carefully-chosen four measurements – we would have all the same counts from $S_1 - S_4$ so that we would not have enough information to discern four blocks. It could be proven mathematically as well since the reduced 4×4 matrix for $S_1 - S_4$ has three linearly independent rows, i.e., its rank is three, so we end up having an under-determined system. This conundrum with four equations and four unknowns are solved if we substitute one of the signals with a measurement in the diagonal direction, S_5 or S_6.

Therefore, we could estimate $\Sigma_1 - \Sigma_4$, using either an inverse matrix of 4×4 matrix based on four measurements ($S_1 - S_3$ and S_5 (diagonal)) or a pseudo-inverse of matrix A above, which includes all the possible six measurements. The bubble counts $S_1 - S_6$ and neutron flux ϕ_0 were calculated from MCNP6.2[4] and Σ_{poly} from ENDF/B-VII.1 library.[5] To get the bubble counts, we convolved the MCNP-calculated neutron flux with the response curve of C318 bubble detector at the temperature 25°C.[6] We assumed running the D-T generator of the EXCALIBUR at the current of 70 μA and the voltage of 130 kV for 10 minutes, which theoretically gives us the source rate of 5.07×10^8 neutrons/s.

Preliminary experiment set-up

We set up the preliminary experiment for 2D radiographs at PPPL as shown in Figure 4.

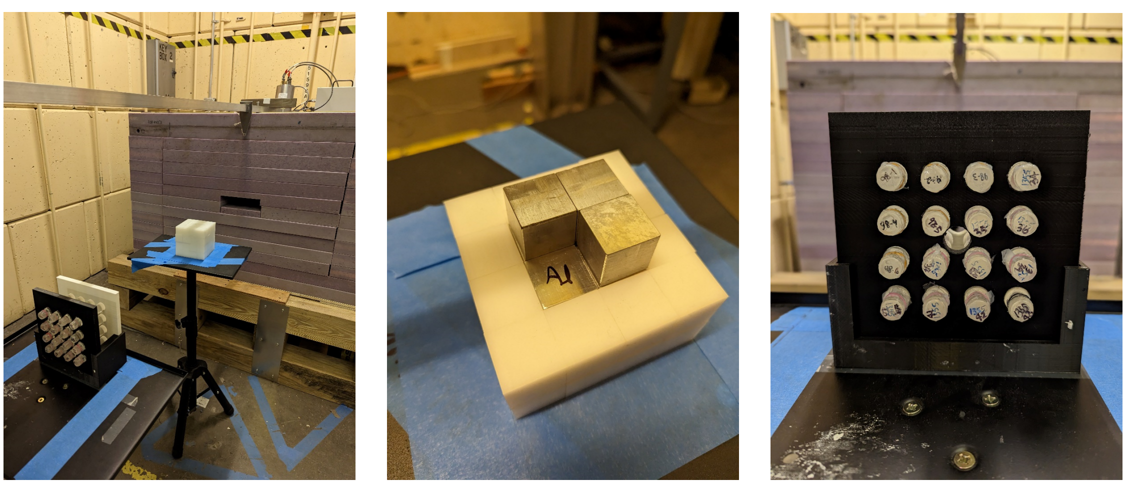

Figure 4: (Left) View from the back of the bubble detectors in a (4×4) grid looking at a (4×4×4) voxel target and the EXCALIBUR neutron source. (Middle) Inside the target with stainless steel and aluminum blocks. (Right) Back of the bubble detectors in a (4×4) grid.

We ran the EXCALIBUR at the current of 70 μA and the voltage of 130 kV for 4 minutes. From this run, we didn't have enough bubbles to make a statistically sound conclusion, not only because we had a shorter exposure time than we set for MCNP but also we didn't take into consideration of detector calibration in the calculation. We continue to work on more neutron exposures and generate the calibration data of bubble detectors.

Results

The calculated results are shown in Table 1. In case 1 where all blocks were stainless steel, we could find that the standard deviation of the cross-section of four SS blocks is lower when we used 6 signals instead of 4 signals. In the ideal case, the cross-section of stainless steel and aluminum would be 0.569 inch^{-1} and 0.267 inch^{-1} based on the total neutron cross-section at 14 MeV from ENDF/B-VII.1 library.[5] Also, in case 3, the difference between SS and Al increased with 6 measurements compared to that with 4 measurements.

Table 1: Calculated cross-section of four blocks in case 1-3. Units in inch^{-1}. Actual material for the block is either stainless steel (SS) or aluminum (Al). 4 signals used were S_1, S_2, S_3 and S_5 and 6 signals were $S_1 - S_6$ in Figure 3.

	Cross-section in case 1			Cross-section in case 2			Cross-section in case 3		
	Mat.	4 signals	6 signals	Mat.	4 signals	6 signals	Mat.	4 signals	6 signals
Σ_1	SS	0.477	0.499	Al	0.214	0.225	SS	0.453	0.474
Σ_2	SS	0.562	0.495	SS	0.537	0.503	Al	0.316	0.261
Σ_3	SS	0.570	0.503	Al	0.276	0.237	Al	0.316	0.273
Σ_4	SS	0.477	0.499	SS	0.494	0.509	SS	0.453	0.462

We also calculated the ideal bubble counts which can be expected with the ideal cross-section values, as shown in Table 2. In overall, ideal counts were around 10% less than MCNP calculation and it showed more difference especially for the measurements at the diagonals (S_5 and S_6). It is not surprising since the linear algebraic model assumes the neutron path connecting a point source with a point detector and it gives us the maximum path length, especially at the diagonals. The actual neutron source in the D-T generator is a tritiated target with a radius of 0.5 cm and the actual bubble detector has a radius of 0.5 cm. The neutron beam is expected to have a width of ~1.44 cm at the center of the Rubik's cube. Thus, for example, the diagonal measurement from S_5 in case 3 will have much less attenuation in Monte Carlo simulation than the simple algebraic model because of the fact that not only there are neutrons going through the path length shorter than the maximum length from the model but also there will be some neutrons going through aluminum blocks which is not expected in the model. Beside this geometric effect, neutron scattering will also make an object look less attenuating than the total cross-section suggests since many of those scattered neutrons in the object or surroundings will end up interacting at the bubble detector.

Table 2: Bubble counts in the signal $S_1 - S_6$ from MCNP and from ideal calculation. Ideal calculation shows the estimated bubble counts when we assume the cross-section of stainless steel and aluminum as 0.569 inch^{-1} and 0.267 inch^{-1} based on the total neutron cross-section at 14 MeV from ENDF/B-VII.1 library.

	Bubble counts in case 1			Bubble counts in case 2			Bubble counts in case 3		
	MCNP	Ideal	Diff	MCNP	Ideal	Diff	MCNP	Ideal	Diff
S_1	123	111	12	164	150	14	161	150	11
S_2	122	111	11	161	150	11	161	150	11
S_3	122	111	11	213	203	10	161	150	11
S_4	123	111	12	123	111	12	165	150	15
S_5	72	55	17	102	85	17	77	55	22
S_6	72	55	17	101	85	16	136	130	6

Conclusions

In this study, for the first time, we conducted calculations and preliminary experiments with a test object with 3D structure combined with 2D radiography for the application of zero-knowledge protocol (ZKP). This 2D imaging system with 3D objects enables more realistic zero-knowledge protocol studies.

The MCNP calculation showed the results as we expected. In theory, we can distinguish the 1" cube of SS and Al even with the simple analytic model. However, the model needs to be further improved due to the finite size neutron source and the finite size detector since the signal at the diagonals picked up neutron attenuation from adjacent blocks. We will further study the statistical uncertainty of this approach to figure out optimal bubble counts for ZKP application.

We are working on more neutron exposures and generating the calibration data for bubble detectors. We will continue to improve bubble counting algorithms for the better imaging analysis with less uncertainties. We will perform more proof-of-concept experiments for this differential radiography at PPPL in the near future.

Acknowledgements

This work was supported by the U.S. Department of Energy under contract number DE-AC02-09CH11466. The United States Government retains a non-exclusive, paid-up, irrevocable, world-wide license to publish or reproduce the published form of this manuscript, or allow others to do so, for United States Government purposes. This work is also supported by the U.S. Department of Energy, National Nuclear Security Administration, Office of Defense Nuclear Nonproliferation Research and Development.

References

1. Glaser, A., Barak, B., Goldston, R. A zero-knowledge protocol for nuclear warhead verification. Nature 510, 497–502 (2014).

2. Philippe, S., Goldston, R., Glaser, A. et al. A physical zero-knowledge object-comparison system for nuclear warhead verification. Nature Communications 7, 12890 (2016).

3. Gilson, E., Glaser, A., Goldston, R., et al. "The EXCALIBUR Neutron Source – Characterization and Current and Planned Operational Modes", Proceedings of 63rd Annual Meeting of Institute of Nuclear Material Management (2022).

4. Werner, C., et al., "MCNP6.2 Release Note", Los Alamos National Laboratory, report LA-UR-18-20808 (2018).

5. Chadwick, M., Herman, M., Obložinský, P., et al., "ENDF/B-VII.1: Nuclear Data for Science and Technology: Cross Sections, Covariances, Fission Product Yields and Decay Data", Nuclear Data Sheets 112, 2887 (2011).

6. d'Errico, F., Radiation dosimetry and spectrometry with superheated emulsions, Nuclear Instruments and Methods in Physics Research B 184, 229-254 (2001).